Hypersonic Viscous-Inviscid Interaction with Vectored Surface Mass Transfer

G. R. Inger* and T. F. Swean†
Virginia Polytechnic Institute and State University, Blacksburg, Va.

A fundamental theoretical study of homogeneous vectored injection and suction in two-dimensional or axisymmetric high-speed flows with heat transfer and self-induced pressure gradients is described, based on local similarity solutions of the laminar boundary-layer equations. The results show the important effects of both injection velocity and vector angle on a variety of physical properties of practical interest such as velocity and temperature profiles, skin friction, incipient separation, heat-transfer rate, displacement thickness, and induced pressure field. In addition, new solutions pertaining to upstream-vectored injection are investigated.

Nomenclature

$A,B,D,E,$ = constants in viscous-inviscid interaction effect solutions
C = $\rho_w\mu_w/\rho_{e0}\mu_{e0}$
f_{0w} = normal injection parameter $[-\dot{m}_w(2Re_{x0})^{1/2}/\rho_{e0}\mu_{e0}]$
f'_{0w} = tangential injection parameter $(=u_w/u_{e0})$
g = total enthalpy ratio H/He $(H+h+U^2/2$
$I_{0_{1,2,3}}$ = boundary-layer profile integrals; see Eqs. (18) and (19)
I_c, I_p = boundary-layer solution integrals, see Eq. (25)
J_1 = Hayes-Probstein tangent wedge function
K,L,M = displacement thickness parameters, see Eq. (32)
$\dot{m}_w$ = surface mass transfer rate $(\rho_w v_w)$
M = Mach number
P = static pressure
Pr = Prandtl number
$\dot{q}_w$ = surface heat transfer rate
r_B = body radius
Re_x = $\rho_e u_e x/\mu_e$ (Reynolds number)
$\Re$ = recovery factor, Eq. (29)
T = static absolute temperature
u,v = velocity components in x,y directions
γ = ratio of specific heats
δ^* = boundary-layer displacement thickness $=\int_0^\infty [1-(\rho u/\rho_e u_e)]dy$
ϵ = 0, 1 for two-dimensional and axisymmetric flow, respectively
η = $(u_e r_B{}^\epsilon \int_0^y \rho dy(2\epsilon)^{1/2}$
λ = coefficient of heat conduction
μ = viscosity
ξ = $\int_0^x \rho_e\mu_e r_B{}^{2\epsilon} dx$
ρ = density
τ = shear stress
θ_B = injection angle at surface $(\tan^{-1} v_w/u_w)$
ψ = stream function
$\bar{\chi}$ = $(\rho_w\mu_w/\rho_e\mu_e)^{1/2} M_e^3/(Re_x)^{1/2}$
e = edge of boundary layer (inviscid flow)
w = conditions at wall surface
AD = adiabatic wall flow conditions
∞ = freestream conditions
0 = basic isobaric flow without interaction
1 = interaction-perturbation

Superscripts
$(\,)'$ = $\partial/\partial\eta$

Presented as Paper 75-840 at the AIAA 8th Fluid and Plasma Dynamics Conference, Hartford, Conn., June 16-18, 1975; submitted June 23, 1975; revision received October 20, 1975. Based on research supported by Air Force Office of Scientific Research under Grant 72-2173.

Index categories: Boundary Layers and Convective Heat Transfer – Laminar; Supersonic and Hypersonic Flows.

*Professor, Aerospace and Ocean Engineering Department. Associate Fellow AIAA.

†Graduate Research Assistant, Aerospace and Ocean Engineering Department. Member AIAA.

I. Introduction

THE theoretical study of surface mass transfer effects involving both normal and tangential components ("vectored" suction or injection) is an important flow problem associated with the film cooling of hypersonic transport aircraft, the transpiration cooling protection of entry vehicles and rocket nozzles, the use of suction and blowing for boundary-layer control, separation delay, and inducing control forces on aerodynamic vehicles, and studies of high-altitude (low-density) surface slip and temperature jump effects on mass transfer and heat transfer in rarefied flows. Very few investigations of this problem have been made, these being limited to low-speed adiabatic flows and only a small part of the injection velocity and angle range of practical interest. This situation has been improved recently by a comprehensive study of similarity solutions for homogeneous vectored injection and suction in nonadiabatic laminar boundary layers with zero axial pressure gradient.[1] However, in the aforementioned hypersonic flow applications, it is known that the self-induced pressure gradient effects caused by the boundary-layer displacement thickness growth are significant; moreover, these effects can be greatly enhanced by the presence of surface mass transfer.[2]

This paper describes the results of an analytical investigation of the effects of vectored surface mass transfer into nonadiabatic hypersonic laminar boundary-layer flow in the presence of viscous-inviscid interaction. Our approach treats the interaction effects as small perturbations on a basic locally-similar isobaric flow, and as such constitutes a two-fold extension of previous work: a) it extends the existing theory of normal blowing for strong-interaction flows[3] into the "weak-to-moderate" interaction regime; and b) it considers for the first time the influence of *vectored* blowing and suction in a pressure gradient.

Sec. II shows that the problem can be split approximately into two parts, a basic self-similar isobaric flow solution with heat transfer, plus a small nonsimilar perturbation caused by the self-induced axial pressure gradient. Sec. III then describes the solution of these two problems, including both analytical and numerical results. The discussion shows the influence of vectored injection and suction on various properties of practical interest, such as boundary-layer velocity and temperature profiles, skin friction, heat transfer, recovery factor, displacement thickness, and the induced pressure field. These solutions yield valuable insight and a first ap-

proximation to the influence of vectored suction and injection on high-speed flows and viscous-inviscid interaction. Furthermore, they provide useful basic elements for constructing more general approximate solution methods such as an integral method approach. Also studied are a new branch of solutions pertaining to certain ranges of *upstream* mass transfer vectoring without flow reversal. Finally, Sec. IV presents an example application of the theory.

II. Formulation of the Analysis

We consider steady laminar flow past a two-dimensional or axisymmetric surface, taken at sufficiently high Reynolds number to justify use of boundary-layer theory. To simplify the analysis down to the essential physical features of interest, the following approximations are introduced. The basic boundary-layer flow without interaction is locally-similar with longitudinal surface curvature effects and the so-called transverse curvature effect associated with slender axisymmetric bodies both neglected. A perfect gas of the same type as the mainstream can be injected through the surface (e.g., the surface may be porous); the two are assumed not to react, however. The density-viscosity product $\rho\mu$ is assumed constant across the boundary layer, as is the Prandtl number Pr (nonunity values of Pr are considered, however). Finally, the local inviscid flow is assumed to be hypersonic and isobaric except for pressure gradients induced by weak viscous-inviscid interaction. This interaction, which is caused by the first-order boundary-layer displacement effect on the inviscid flow, is represented by the tangent-wedge (or tangent-cone) approach, an approximation which yields good engineering accuracy in a convenient closed form. Thus, adapting the general analytical procedure described in Ref. 4 to the present problem, the leading approximation to the pressure field is of the form

$$p_e/p_{e0} \simeq 1+\gamma E\bar{\chi}_0 \tag{1}$$

where the parameter E depends on the boundary-layer and inviscid flow solutions as shown below and $\bar{\chi}_0$ is the fundamental viscous-interaction parameter (see Nomenclature), here assumed small compared to unity.

We introduce a stream function $\psi=(2\xi)^{1/2}f(\xi,\eta)$ in terms of the Levy-Lees similarity variables

$$\eta=(u_e r_B^{\epsilon}\int_0^y \rho dy)/(2\xi)^{1/2}, \xi=\int_0^x \rho_w\mu_w u_e r_B^{2\epsilon}dx$$

where $\epsilon=0$, 1 for two-dimensional and axisymmetric flow, respectively, plus the dependent variables $u/u_e=\partial f/\partial\eta\equiv f'$ and $g=H/H_e$ with $H=h+(u^2/2)$. The pressure field induced along the body by weak viscous inviscid interaction is given in the first approximation by

$$\frac{p_e}{pe_0} \simeq 1+\gamma E\bar{\chi}_0+0(\bar{\chi}_0^2)+\ldots$$

$$=1+\gamma M_\infty J_1\left(\frac{v_e}{u_e}\right)+0(\bar{\chi}_0^2)+\ldots \tag{2}$$

where $J_1(M_\infty)$ is the tangent wedge function defined by Hayes and Probstein ($=1$ when $pe_0=p_\infty$, i.e., a flat plate) and the subscript "0" denotes the original noninteracting flow conditions (both inviscid and viscous), and where the deflection angle of the boundary-layer displacement thickness δ_0^*, including the presence of surface mass transfer $\dot{m}_w$, is given by the integrated continuity equation as

$$\left(\frac{v_e}{u_e}\right)_0 \simeq \frac{d\delta_0^*}{dx}+\frac{\dot{m}_w}{\rho_{e_0}u_{e_0}} \tag{3}$$

All the other inviscid properties are expressed in a like manner, giving the isentropic relations

$$\frac{u_e}{u_{eo}} \cong 1-\frac{E}{M_{e0}^2}\bar{\chi}_0+0(\bar{\chi}_0^2)+\ldots \tag{4a}$$

$$\frac{T_e}{T_{e0}} \cong 1+(\gamma-1)E\bar{\chi}_0+0(\bar{\chi}_0^2)+\ldots \tag{4b}$$

where we note that $H_e=H_{e0}$, $\xi/\xi_0\simeq 1+2E(\gamma M_{e0}^2-1)M_{e0}^{-2}\bar{\chi}_0$ and that $u_{e0}^2/2\ H_e=1+[2M_{w0}/(\gamma-1)]$ is near unity for local hypersonic flow. Correspondingly we expand the boundary-layer property variables in an analogous form as follows

$$f(\xi,\eta)\simeq f_0(\eta)+\left[\left(\frac{\gamma-1}{2}\right)+M_{e0}^{-2}\right]Ef_1(\eta)\bar{\chi}_0+\ldots \tag{5}$$

$$g(\xi,\eta)\simeq g_0(\eta)+\left[\left(\frac{\gamma-1}{2}\right)+M_{e0}^{-2}\right]Eg_1(\eta)\bar{\chi}_0+0(\bar{\chi}_0^2)+\ldots \tag{6}$$

where f_0 and g_0 pertain to the basic self-similar isobaric flow, while f_1 and g_1 are perturbations because of the self-induced pressure gradient. Substituting the foregoing expansions and assumptions into the general boundary-layer momentum and energy equations and neglecting terms of order $\bar{\chi}_0^2$, one obtains, after considerable algebra,[5] the following two sets of ordinary differential equations governing the basic and perturbation fields, respectively:

$$f_0'''+f_0f_0''=0 \tag{7}$$

$$g_0''+Prf_0g_0+(Pr-1)(U_{e0}^2/2H_e)(f_0'^2)''=0 \tag{8}$$

$$f_1'''+f_0f_1''+f_0'f_1'=f_0'^2-g_0 \tag{9}$$

$$g_1''+Pr(f_0g_1'+f_0'g_1)+u_{e0}^2/H_e)(Pr-1)(f_0'f_1')''$$
$$+(1-Pr)(u_{e0}^2/H_e)[(u_{e0}^2/2H_e)-1](f_0'^2)''=0 \tag{10}$$

The corresponding boundary conditions required to insure matching with the disturbed inviscid flow at the outer edge of the boundary layer are that $f_0'(\infty)=g_0(\infty)=1$ and $f_1'(\infty)=0$, whereas the continuum boundary conditions at the wall of known surface temperature with both normal and tangential injection present are

$$f_0(0)=-\sqrt{2\xi_0}\ \dot{m}_w/\rho_{e0}u_{e0}\mu_{e0}r_B^{\epsilon}\equiv f_{0w}\ \text{(given)} \tag{11}$$

$$f_0'(0)=u_w/u_{e0}\equiv f_{0w}'\ \text{(given)} \tag{12}$$

$$g_0(0)=(h_w/H_e)+(u_{e0}^2/2H_e)(f_{0w}')^2$$
$$\equiv g_{0w}(h_w\ \text{given}) \tag{13}$$

and

$$f_1(0)=g_1(0)=0 \tag{14}$$

$$f_1'(0)=f_{0w}'[1-u_{e0}^2/2H_e)] \tag{15}$$

Here f_{0w} and f_{0w}' represent the nondimensional normal and tangential injection velocities at the surface, respectively, being negative constants for blowing and upstream vectoring, respectively. It is seen that the zero- and first-order solutions are each influenced by both these injection parameters. A schematic illustration of the four different physical cases of mass transfer considered is shown in Fig. 1. In terms of the parameters f_w and f_w', the actual resultant injection velocity

and its vector angle θ_B, with the respect to the wall, are given by

$$(u_w/u_e)^2+(v_w/u_e)^2=$$

$$(f_w')^2+T_w{}^2f_w{}^2(\partial\xi/\partial x)2Re_x[(\xi/x)T_e^2]^{-1}$$

and

$$\tan\theta_B=-T_wf_w/T_ef_w'[2Re_x(\xi/x)dx/d\xi]^{1/2}$$

respectively. This latter equation indicates that the addition of just a moderate amount of tangential injection in a high Reynolds number flow reduces the angle θ_B to very small values even in the presence of large normal mass transfer, especially on a cold wall ($T_w \ll T_e$).

Once the previous boundary value problems are solved, the important gross physical properties can be evaluated from the following relations:

Shear Stress

$$\frac{(2\xi_0)^{1/2}\tau_w}{C_w\rho_{e0}\mu_{e0}u_{e0}{}^2r_B^\epsilon}\simeq f_{0w}''+E\bar{\chi}_0\left\{\left[\left(\frac{\gamma-1}{2}\right)+M_{e0}{}^{-2}\right]f_{1w}''-f_{0w}''M_{e0}{}^{-2}\right\} \tag{16}$$

Heat Transfer

$$\frac{(2\xi_0)^{1/2}\dot{q}_w}{\rho_{e0}\mu_{e0}u_{e0}H_er_B^\epsilon}=(h'/H_e)_w+Pr(u_e^2/H_e)(f_w'f_w'') \tag{17a}$$

$$\simeq g_{0w}'+(Pr-1)(u_{e0}{}^2/H_e)f_{0w}'f_{0w}''+E\bar{\chi}_0\left\{\left[\frac{\gamma-1}{2}+M_{e0}{}^{-2}\right]g_{1w}'+(Pr-1)(u_{e0}{}^2/H_e)f_{0w}'\left[f_{1w}''\left[\frac{\gamma-1}{2}+M_{e0}{}^{-2}\right]-f_{0w}''M_{e0}{}^{-2}\right]\right\} \tag{17b}$$

where it is noted that the last term in Eq. (17a) derives from the frictional heating $\tau_w u_w$ associated with the tangential velocity component at the surface.

Displacement Thickness

$$\frac{\rho_{e0}u_{e0}r_B^\epsilon\delta^*}{(2\xi_0)^{1/2}}\simeq\underbrace{\int_0^\infty(g_0-f_0')\,d\eta}_{I_{01}}+U_{e0}{}^2/2h_{e0})\underbrace{\int_0^\infty(g_0-f_0'{}^2)\,d\eta}_{I_{02}}+E\bar{\chi}_0\left[\left(\frac{\gamma-1}{2}\right)+M_{e0}{}^{-2}\right]\left\{\int_0^\infty(g_1-f_1')\,d\eta+(u_{e0}{}^2/2h_{e0})\left[\int_0^\infty(g_1-2f_0'f_1')\,d\eta-2I_{02}\right]\right\} \tag{18}$$

Momentum Thickness

$$\frac{\rho_{e0}u_{e0}r_B^\epsilon\theta^*}{(2\xi_0)^{1/2}}=\underbrace{\int_0^\infty f_0'(1-f_0')\,d\eta}_{I_{03}}+E\bar{\chi}_0\left[\left(\frac{\gamma-1}{2}\right)+M_{e0}{}^{-2}\right]\int_0^\infty f_1'(1-2f_0')\,d\eta \tag{19}$$

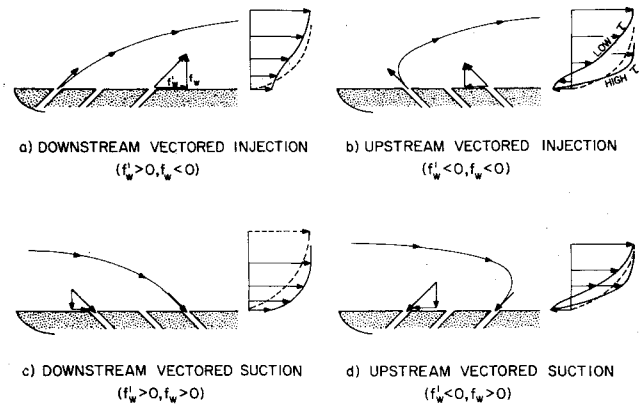

Fig. 1 Flow configurations with vectored mass transfer (schematic).

It is easily shown that the following relationship exists between the three integrals defined in Eqs. (18) and (19):

$$I_{02}=I_{01}+I_{03} \tag{20}$$

where it should be noted that I_{03} is independent of both wall temperature and Pr.

Induced Pressure

The basic parameter E in Eqs. (1), (2) is found to be given by

$$E=\left[M_\infty J_1(M_\infty)/(2)^{1/2}M_{e0}\right]\left[\left(\frac{\gamma-1}{2}\right)I_{02}+M_{e0}{}^{-2}(I_{01}-f_{0w})\right] \tag{21a}$$

$$=(M_\infty J_1/M_{e0})\left\{\left(\frac{\gamma-1}{2}\right)\left(I_0/(2)^{1/2}\right)+\left[\frac{\gamma-1}{2}+M_{e0}{}^{-2}\right]\left(I_{01}/(2)^{1/2}\right)-\frac{f_{0w}}{\sqrt{2}}M_{e0}{}^{-2}\right\} \tag{21b}$$

III. Solution Results and Discussion

Equations (7) and (8) governing the basic zero-order flow have been solved by numerous investigators for zero or normal mass transfer; more recently solutions have been given by the present authors for a wide range of nonadiabatic tangential mass transfer conditions in low-speed isobaric flows.[1] For the present study these solutions have been extended to include the hypersonic interacting case. It suffices here to say that these equations are easily solved numerically by the standard shooting technique used in two-point boundary value problems of the boundary-layer type. Linear equations similar to our first perturbation Eqs. (9) and (10) have been solved by Maslen[6] for slip flow on a flat plate and by Lees and Probstein[7] for hypersonic, weak interacting boundary-layer flow with zero mass transfer; completely analytical solutions to these equations can thus be readily obtained. A detailed discussion of all these results, including complete tabulation of the solutions, is given in Ref. 5; selected features will be discussed in the following paragraphs.

A. Velocity Field

The zero-order noninteracting component of the flow has already been described.[1] It was shown there that when the normal injection velocity is less than the Emmons-Leigh[8] critical blow-off value ($f_{0w}=-0.87574$), solutions exist for a limited range of *upstream* tangential injection velocities which are double-valued with high- and low-positive wall-shear values, respectively.[9,10] These solutions are reminiscent of the double-valued solution branch obtained by Cohen and

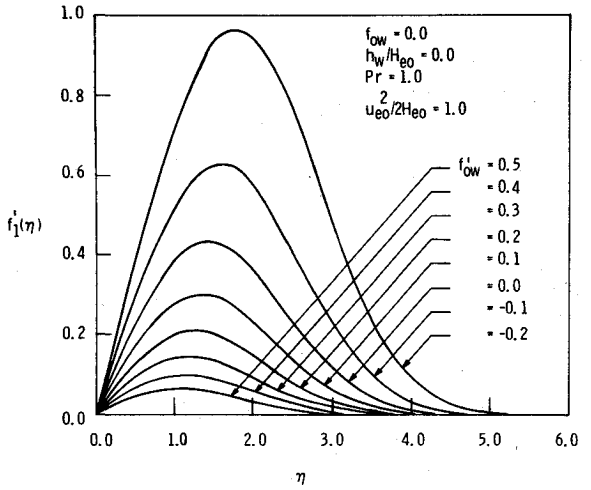

Fig. 2 Tangential injection effect on perturbation velocity profiles.

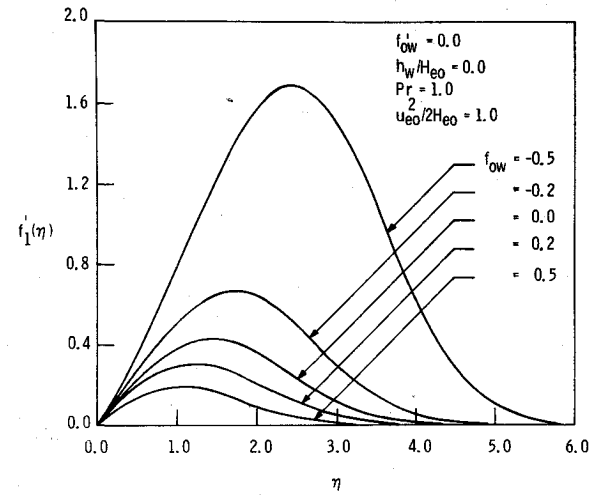

Fig. 3 Normal injection effect on perturbation velocity profiles.

Reshotko[11] in their well-known of pressure gradient effects on self-similar boundary-layer flows, and may be physically explained in terms of dissimilar upstream history effects following their arguments and those of Libby and Liu.[12] On the other hand, solutions are also possible for "supercritical" blowing with nonvanishing downstream tangential injection, all of which are single-valued.

The first-order perturbation flow due to viscous interaction governed by the linear Eq. (9) can be solved analytically in terms of straightforward quadratures of the known basic solution f_0, g_0. Omitting the details,[5] the following solution is found to satisfy the stated boundary conditions:

$$f_1'(\eta) = f_0'' \left\{ \int_0^\eta \left[I_{02}(\infty) - I_{02}(\eta) \right] (f_0'')^{-1} d\eta + \left[1 - (u_{e0}^2/2H_e) \right] (f'_{0w}/f''_{0w}) \right\} \tag{22}$$

with

$$f''_{1w} = I_{02} - f_{0w} f'_{0w} (1 - u_{e0}^2/2H_e) \tag{23}$$

Some typical first-order velocity profiles from this solution are shown in Figs. 2-4. Figures 2 and 3 illustrate the effects of the tangential and normal mass transfer rates, respectively: note that the interaction-induced velocities are increased by upstream tangential injection ($f'_{0w} < 0$) and normal blowing ($f_{0w} < 0$), and diminished by downstream tangential injection or suction. The wall temperature has a significant influence on the solution as shown in Fig. 4, which compares typical

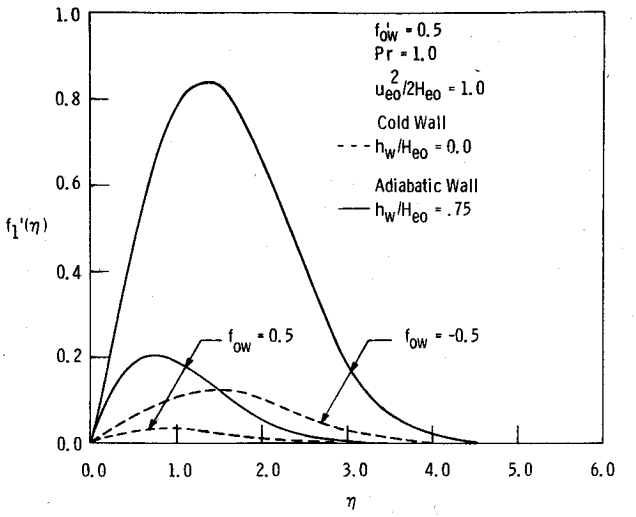

Fig. 4 Wall temperature effect on perturbation velocity field.

profiles for both a cold wall and an adiabatic wall. Owing to the enhanced influence of pressure gradient with lower density, the perturbation velocities increase significantly with wall temperature ratio. The Prandtl number effect was found to be very small, however.

In Figs. 5 and 6, the wall shear perturbation f''_{1w} is plotted as a function of the tangential injection velocity f'_{0w} with the normal velocity at the surface f_{0w} as a parameter. These figures show the increased shear perturbations associated with blowing and upstream tangential injection: note also the double-valued solutions for upstream tangential injection corresponding to the basic noninteracting solutions.[1] Equation (23) shows that for zero mass transfer or $u_{e0}^2/2H_{e0} = 1.0$ the shear perturbation is equal to the displacement thickness integral I_{02}. Figures (6a) and (6b) show that increasing the wall temperature greatly increases the perturbation flow. Indeed for upstream injection at large blowing velocities and higher wall temperatures, it is seen that $f''_1(0)$ becomes large compared to unity and the first-order perturbation approach breaks down.

B. Enthalpy Field

A formal solution of Eq. (8) governing the zero-order total enthalpy field in terms of quadratures of the velocity field can be obtained for arbitrary Pr and g_w by the standard method of complementary and particular integrals, as follows:

$$g_0(\eta, Pr) = g_{w0} + (1 - g_{w0}) \frac{I_c(\eta, Pr)}{I_c(\infty, Pr)} - (1 - Pr) \frac{u_e^2}{2H_e} \times \left[\frac{I_c(\eta, Pr)}{I_c(\infty, Pr)} \cdot I_p(\infty, Pr) - I_p(\eta, Pr) \right] \tag{24}$$

where

$$I_c \equiv \int_0^\eta (f_0'')^{Pr} d\eta \tag{25a}$$

$$I_p \equiv \int_0^\eta (f_0'')^{Pr} \left[\int_0^\eta (f_0'')^{-Pr} (f_1'^2)'' d\eta \right] d\eta \tag{25b}$$

In the special but important case of $Pr = 1$, these integrals can be completed analytically for arbitrary vectored mass transfer, yielding

$$I_c(\eta, Pr = 1) = (f_0' - f'_{0w})/(1 - f'_{0w}) \tag{26a}$$

$$I_p(\eta, Pr = 1) = \tfrac{1}{2}(f_0'^2 - f'^2_{0w}) + f_0 f_0'' - f_{0w} f''_{0w} + (f_{0w}^2 - 2f'_{0w})(f_0' - f'_{0w}) \tag{26b}$$

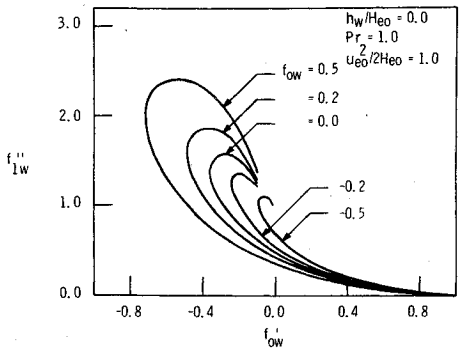

Fig. 5 Influence of mass transfer vectoring on wall shear stress perturbation due to viscous interaction.

and thus giving the following generalized Crocco-type energy equation integral for all types of tangential and normal velocities at the surface:

$$g_0(\eta, Pr=1) = g_{w0} + (1-g_{w0})\left(\frac{f'_0 - f'_{0w}}{1-g'_{0w}}\right) \tag{27}$$

It is seen from these equations that when Pr is near unity the $(g_0 - g_{0w})/(1-g_{w0})$ profiles are similar to the zero-order velocity profiles previously described.

The enthalpy gradient at the wall is obtained by differentiation of Eq. (24) as

$$g'_0(0,Pr) = \frac{I'_c(0,Pr)}{I_c(\infty,Pr)}\left[1 - g_{w0} - (1-Pr)\frac{u_{e0}^2}{2H_e} I_p(\infty,Pr)\right] \tag{28a}$$

$$g'_0(0,Pr=1) = (1-g_{0w}) f''_{0w}/(1-f'_{w0}) \tag{28b}$$

Values of the basic parameters $I'_c(0,Pr)/I_c(\infty,Pr)$ and $I_p(\infty,Pr)$ are tabulated along with f''_{0w} as a function of f_{0w} and f'_{0w} in Table 1. The typical influence of vectored mass transfer on g'_{0w} follows the same trend (including double valued upstream vectoring) as the wall shear.[1]

The adiabatic recovery factor for $\dot{q}_{w0} = 0$ in the noninteracting flow is obtained from Eqs. (13), (17b) and (28a) as

$$\mathcal{R}_0 \equiv \frac{h_{w0,AD} - h_{e0}}{u_{e0}^2/2} = 1 - f'^2_{0w} - (1-Pr)\frac{u_{e0}^2}{2H_e} \times \left[I_p(\infty) + \frac{I_c(\infty)}{I'_c(0)} f'_{0w} f''_{0w}\right] \tag{29}$$

As is well-known, there is no effect of normal mass transfer on the recovery factory when $Pr=1$; however, there is a reduction associated with the tangential injection term which in high-speed flows may be significant.

Regarding the interaction-perturbed enthalpy field governed by the linear Eq. (8), its solution subject to boundary conditions $g_1(\infty) = g_1(0) - 0$ is found to be

$$g_1(\eta) = (1-Pr)(u_{e0}^2/H_e)(f''_0)^{Pr}\int_0^\eta \left\{f'_0 f''_1 + f''_0 f'_1 + \left[(u_{e0}^2/2H_e) - 1\right] 2 f'_1 f''_0\right\}(f''_0)^{-Pr} d\eta \tag{30}$$

with

$$g'_1(0) = (1-Pr)(u_{e0}^2/H_e) f'_{0w}\left[f''_{1w} + f''_{0w}\left(\frac{u_{e0}^2}{2H_e} - 1\right)\right] \tag{31}$$

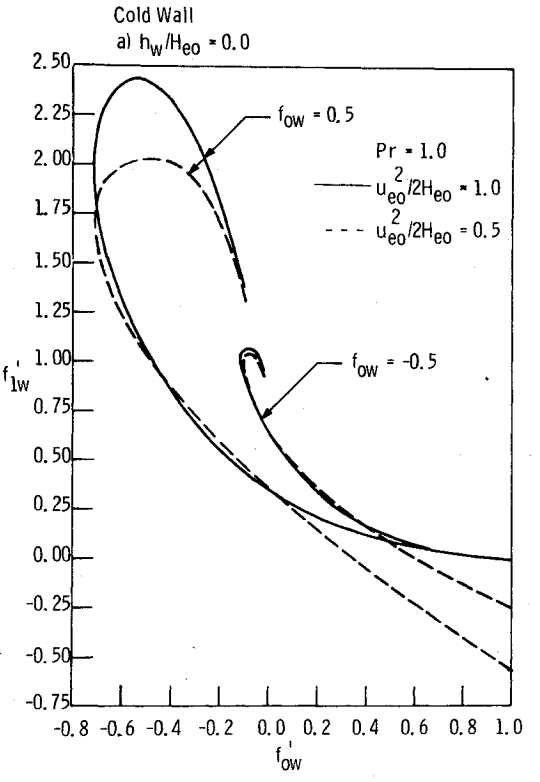

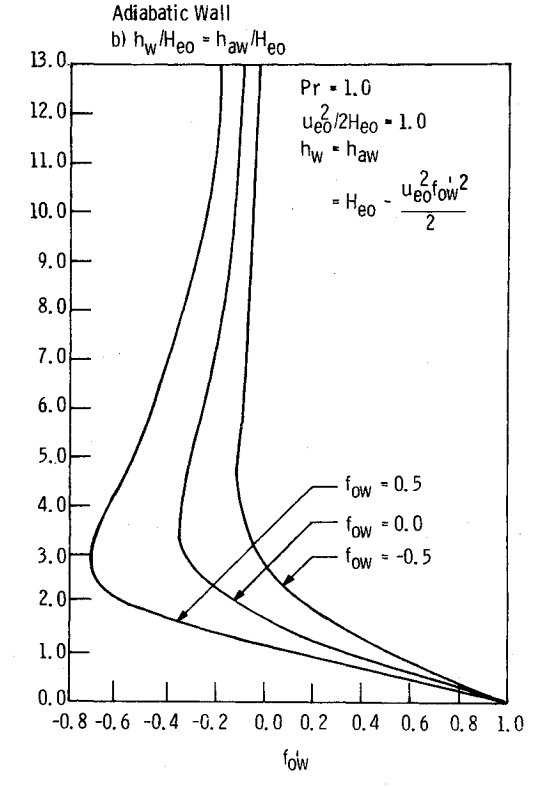

Fig. 6 Wall temperature effect on shear stress perturbation.

As expected, the total enthalpy perturbation vanishes regardless of the magnitude or direction of the surface mass transfer when $Pr=1$. Some typical $g_1(\eta)$ profiles for $Pr=0.70$ are shown in Fig. 7. The effects of the wall parameters f'_{0w}, f_{0w}, and h_w/H_e are found to be analogous to those for $f'_1(\eta)$ previously discussed.

Inspection of Eq. (31) shows that both $g'_1(0)$ and the net first-order heat transfer perturbation coefficient of $E\dot{\chi}_0$ in Eq. (17b) are proportional to the product $(1-Pr)f'_{w0}$; thus we see

Table 1 Tabulation of boundary-layer solution results with vectored blowing and suction

f_{ow}	f_{ow}'	f_w''	I_{03} (b)	$I_p(\infty)$ (c)	N	Pr = 1.00 K (a)	A	B	D	Pr = 0.70 K	A	B	D
f_w=.2	f_w'=-.1	0.6323	0.4123	0.1925	-0.0367	1.0999	0.7779	0.1458	0.5348	1.2450	0.8805	0.1497	0.5645
		0.0002	-0.2591	0.3190	0.0337	13.6490	9.2280	-0.0916	4.5220	13.5580	9.5880	-0.0953	4.2430
	=0	0.6190	0.4190	0.4162	0.1930	1.0349	0.7319	0.1482	0.5142	1.1700	0.8274	0.1277	0.4897
	=.2	0.5568	0.3968	0.0806	-0.0180	0.9380	0.6634	0.1403	0.4720	1.0200	0.7214	0.1422	0.4942
	=.4	0.4578	0.3378	-0.1276	-0.4090	0.8671	0.6132	0.1194	0.4260	0.8200	0.5799	0.1628	0.4638
f_w=0	f_w'=-.15	0.4490	0.4490	0.2750	-0.1040	1.8921	0.9852	0.1588	0.6514	1.4250	1.0078	0.1698	0.6321
		0.0086	0.0086	0.2750	0	8.0440	5.6888	0.0030	2.8470	8.0442	5.6890	0.0030	2.6130
	=0	0.4696	0.4696	0.5000	0.2257	1.2167	0.8605	0.1661	0.5964	1.3430	0.9498	0.1422	0.5459
	=.2	0.4431	0.4431	0.1600	-0.0203	1.0724	0.7584	0.1567	0.5359	1.1350	0.8027	0.1589	0.5410
	=.4	0.3751	0.3751	-0.0600	-0.4593	0.9747	0.6893	0.1326	0.4773	0.8900	0.6294	0.1813	0.5017
f_w=-,2	f_w'=-.1	0.2985	0.5185	0.3787	-0.0553	1.6666	1.1786	0.1833	0.7726	1.7180	1.2150	0.1892	0.7277
		0.0028	0.2228	0.3196	0	8.8887	6.2860	0.0789	3.2220	8.8887	6.2860	0.0789	2.9210
	=0	0.3305	0.5305	0.6061	0.2587	1.4680	1.0382	0.1876	0.7067	1.5830	1.1195	0.1602	0.6182
	=.2	0.3381	0.4981	0.2596	-0.0268	1.2412	0.8778	0.1761	0.6150	1.2930	0.9144	0.1789	0.6006
	=.4	0.2985	0.4185	0.0237	-0.5208	1.1036	0.7805	0.1480	0.5383	0.9950	0.7037	0.2032	0.5525
f_w=-.5	f_w'=-.1	0.0589	0.6089	0.5520	-0.1877	3.2924	2.3280	0.2153	1.3790	3.3840	2.3930	0.2352	1.2330
		0.0237	0.5737	0.4719	0	4.4669	3.1591	0.2029	1.7820	4.4609	3.1591	0.2029	1.5584
	=0	0.1484	0.6484	0.7992	0.2903	2.1119	1.4936	0.2293	0.9761	2.2145	1.5661	0.1985	0.7938
	=.2	0.2012	0.6012	0.4406	-0.0536	1.5879	1.1230	0.2126	0.7741	1.6730	1.1832	0.2183	0.7317
	=.4	0.1977	0.4977	0.1739	-0.6419	1.3482	0.9535	0.1760	0.6528	1.1950	0.8451	0.2440	0.6445
f_w=-.8	f_w'=0	0.0174	0.8174	1.1539	0.3403	4.1646	2.9453	0.2890	1.7617	4.2150	2.9809	0.2529	1.2274
	=.2	0.0965	0.7365	0.7492	-0.1234	2.1111	1.4930	0.2604	1.0069	2.2100	1.5629	0.2735	0.8793
	=.4	0.1170	0.5970	0.4176	-0.8111	1.6731	1.1832	0.2111	0.8027	1.4750	1.0431	0.2971	0.7533
f_w=-1.0	f_w'=.05	0.0071	0.9571	1.5071	0.3800	4.7379	3.3507	0.3384	2.0140	4.7950	3.3911	0.2981	1.2270
	=.20	0.0489	0.8489	1.0089	-0.2450	2.6102	1.8460	0.3002	1.2230	2.7153	1.9203	0.3262	0.9957
	=.40	0.0759	0.6759	0.6159	-0.9700	1.9452	1.3757	0.2390	0.9269	1.7150	1.2129	0.3418	0.8362

a) $L \cong -f_{wo}' K$

b) $I_c'(0, Pr)/I_c(\infty, Pr) \simeq Pr^{1/3} f_{ow}''/(1 - f_{wo}')$

c) $I_p(\infty) \simeq 1/2(1 - f_{ow}'^2) - f_{ow} f_{ow}'' + (1 - f_{ow}')(f_{ow}^2 - 2f_{ow}')$

that Hayes' and Probstein's earlier conclusion[4] for zero mass transfer that weak viscous-inviscid interaction has no first-order effect on either heat transfer or recovery temperature in fact holds true for arbitrary rates of homogeneous suction or blowing *normal* to the surface ($f_{0w}'=0$) if $Pr \neq 1$ or for *any* orientation as well if $Pr=1$.

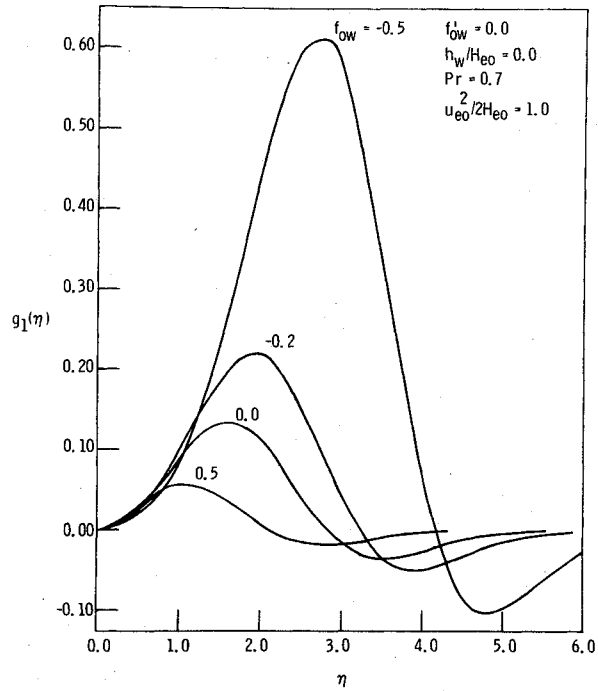

Fig. 7 Typical mass transfer effect on perturbation enthalpy field ($Pr \neq 1$).

C. Momentum and Displacement Thickness

The influence of both downstream and upstream vectored mass transfer on the momentum thickness integral I_{03} defined in Eq. (19), which is independent of Pr and h_w/H_e, is tabulated in Table 1. It is noted that for sufficiently large values of f_w and upstream tangential injection the momentum thickness can be negative.

The zero-order flow displacement thickness integral function I_{01} defined in Eq. (18) can be conveniently decomposed into more fundamental parts by substituting the expression in Eq. (24) for g_0, to obtain

$$I_{01} = g_{0w} \underbrace{\int_0^\infty \left[1 - \frac{I_c(\eta)}{I_c(\infty)}\right] d\eta}_{K(Pr, f_{w0}, f_{w0}')} + \underbrace{\int_0^\infty \left[\frac{I_c(\eta)}{I_c(\infty)} - f_0'\right] d\eta}_{L(Pr, f_{w0}, f_{w0}')}$$

$$- (1 - Pr) \frac{u_{e0}^2}{2H_e} \underbrace{\int_0^\infty I_p(\eta)\, d\eta}_{N(Pr, f_{w0}, f_{w0}')} \tag{32}$$

where the integral parameters K, L, and N so defined have the advantage of being independent of g_{0w} and $u_{e0}^2/2H_e$ and hence may be evaluated once and for all, as opposed to Pr, f_{0w} and f_{0w}' alone‡ (this has been done, the results being tabulated in Table 1.

Regarding the interaction effect on the momentum and displacement thicknesses indicated in Eqs. (18) and (19), it is

‡These functions also have the useful property that

$$K + L = \int_0^\infty (1 - f_0')\, d\eta = \lim_{\eta \to \infty} (\eta - f_0)$$

which is independent of Pr. Note also that for small $(Pr-1)$, $L \simeq -f_{w0}' K$.

found that the coefficients of $E\bar{\chi}_0$ are normally positive (detailed calculation results are given in Ref. 5), and increased by either blowing or upstream vectoring; this implies that the boundary layer is thickened by the induced pressure gradients and by surface mass addition. However, since Eqs. (18) and (19) are of the form $\delta(x)=c_0(x)^{1/2}+Ec_1(x)^{1/2}=\delta_0+d_1$ where d_1 is a constant, we see that such thickening is uniform in x and does not contribute to the slope $d\delta^*/dx$, nor, hence, to the second-order induced pressure regardless of the magnitude or orientation of the surface mass transfer.

D. Useful Engineering Relations for Induced Pressure, Heat Transfer and Skin Friction

With some judicious rearrangement, the key results of the present investigation can be placed in a form that facilitates their direct engineering application in hypersonic aerodynamics.

Induced Pressure

Considered first is the induced pressure parameter E given by Eqs. (2) and (21b). If in this equation we substitute the value of I_{01} from Eq. (32) followed by the expression in Eq. (13) for g_{0w} and writing $u_e^2/2H_e$ in terms of M_{e0}^2, then upon using $L\simeq -f'_{0w}\cdot K$ and neglecting terms of M_{e0}^{-4} and higher we obtain after considerable algebra the following expression pertaining to *arbitrary wall temperature*:

$$p_e/p_{e0}\simeq 1+\gamma\bar{\chi}_0 E \tag{33a}$$

with

$$E\simeq\frac{M_\infty J_1}{M_{e0}}\left\{(\gamma-1)\left[B-\frac{A}{2}f''_{w0}(1-f'_{w0})\right]-M_{e0}^{-2}\left[A\left(\frac{T_w}{T_{e0}}-f'_{0w}\right)-\frac{f_{0w}}{(2)^{1/2}}\right]\right\} \tag{33b}$$

where $A=K/(2)^{1/2}$ and $B=[I_{03}/2(2)^{1/2}-(1-Pr)N/2(2)^{1/2}$. This equation is a direct generalization of Hayes and Probstein's zero mass transfer result (pp. 344-345, Ref. 4) to the general case of arbitrary-vectored blowing or suction. The parameters A and B along with K and D, which depend only on Pr, f_{0w} and f'_{0w}, are tabulated in Table 1; we note that in the absence of mass transfer A and B as defined are exactly equal to the values quoted in Ref. 4. Repeating the derivation using instead the expression $g_{0w}=1-f'^2_{0w}-(1-Pr)(u_{e0}^2/2H_e)[I_p(\infty)+(I_c(\infty)f'_{0w}f''_{0w}/I'_c(0))]$ from Eq. (29) and using $I'_c(0)/I_c(\infty)\simeq f''_{0w}Pr^{1/3}/(1-f'_{0w})$, we obtain the following comparable result for the induced pressure on an *adiabatic wall:*

$$E\simeq\frac{M_\infty J_1}{M_{e0}}\left\{(\gamma-1)\left[D-\frac{A}{2}f''_{w0}[2-Pr^{1/3}(1-f'_{0w})]\right]+M_{e0}^{-2}\left[A(1-f'_{0w})-\frac{f_{0w}}{(2)^{1/2}}\right]\right\} \tag{33c}$$

where $D=B+(A/2)[1-(1-Pr)I_p(\infty)]$ is likewise the generalized mass transfer counterpart of the *H&P* expression and where we have neglected a small term proportional to $(1-Pr)M_{e0}^{-2}$.

Heat Transfer

Introducing Eqs. (13), (21b), and (32) into the general heat transfer expression in Eq. (17b), the following useful relationship is obtained after rearrangement, upon neglecting terms proportional to $(1-Pr)M_{e0}^{-2}$:

$$(2\dot{q}_w/\rho_{e0}u_{e0}H_{e0})Pr^{2/3}\left(\frac{Re_{0x}}{(1+2\epsilon)C_w}\right)^{1/2}\simeq\left(\frac{\sqrt{2}f''_{0w}}{1-f'_{0w}}\right)\times\left\{1-\frac{h_w}{H_e}-\frac{u_{e0}^2}{2H_e}\left[(1-Pr)I_p(\infty)+f'_{0w}[f'_{0w}+2((1-Pr)(1-f'_{0w}]\right]\right\}+8\frac{M_{e0}E^2}{M_\infty J_1}\bar{\chi}_0(1-Pr)f'_{w0}Pr^{-1/3} \tag{34}$$

where all relevant parameters are tabulated in Table 1.

Skin Friction

From Eqs. (20), (21b), and (32) substituted into the shear stress relationship in Eq. (16), there ultimately yields a consistant degree of approximation that

$$C_f\left[\frac{Re_x}{(1+2\epsilon)C_w}\right]^{1/2}\simeq\sqrt{2}f''_{0w}+2\left(\frac{M_{e0}E^2}{MJ_1}\right)\bar{\chi}_0\left\{1+\frac{4[2]^{1/2}}{(\gamma-1)M_{e0}^2}\times\left(B-\frac{[2]^{1/2}f''_{0w}}{8}\right)+\frac{4\sqrt{2}}{(\gamma-1)M_{e0}^2}\left[1-(\gamma-1)\frac{J_1M_\infty}{M_{e0}}\right]\frac{A}{2}\left[\frac{h_w}{H_e}-f'_{0w}(1-f'_{0w})\right]-\frac{f_{0w}}{2[2]^{1/2}}\left[f'_{0w}-(\gamma-1)\times\frac{J_1M_\infty}{M_{e0}}\right]\frac{4(2)^{1/2}}{(\gamma-1)M_{e0}^2}\right\} \tag{35}$$

Displacement Thickness

For the sake of completeness, we include an engineering expression for the zeroth-order displacement thickness. In the foregoing manner we obtain from Eq. (18) the following leading approximation:

$$\frac{\delta_0^*}{x}\left[(1+2\epsilon)\frac{Re_{0x}}{C_w}\right]^{1/2}=2A\left(\frac{T_w}{T_{e0}}-f'_{w0}\right)+\left(\frac{\gamma-1}{2}\right)Me_0^2[4B-2Af'_{0w}(1-f'_{0w})] \tag{36}$$

IV. Illustrative Application

As an example application of the foregoing theory, we consider a cooled flat plate flying in air at an altitude of 100,000

Table 2 Effect of vectored blowing on boundary-layer properties on a flat plate[a]

θ_B, degrees	$\dot{q}_w/(\dot{q}_w)_{\dot{m}_w=0}$	$(p_e/p_\infty)-1$	$C_f/(C_f)_{\dot{m}_w=0}$ $p_e=p_\infty$	$(\Delta C_f/C_{f0})_{\text{INTER}}$	$[\delta^*/x)Re_{0x}/C_w)^{1/2}$
0	1.000	0.157	1.068	0.058	45.7
15	0.806	0.177	0.879	0.072	50.4
30	0.643	0.201	0.737	0.093	55.7
45	0.495	0.224	0.611	0.117	61.2
60	0.389	0.243	0.526	0.138	65.5
75	0.322	0.255	0.476	0.151	68.1
90	0.316	0.258	0.471	0.155	68.8

[a] $x=8$ ft, $M_\infty=15$, 100,000 ft. altitude, $Pr=1$, $g_{0w}=0.20$, $\dot{m}_w/\rho_{e0}u_{e0}=10^{-4}$.

ft at $M_\infty = 15$. Using standard atmospheric properties we find $Re_{x\infty} = 12.9 \times 10^6$ and $\bar{x}_\infty = .943$ at a point 8 ft from the leading edge. Assuming $Pr = 1$ and a wall enthalpy ratio of $g_{w0} \simeq 0.2\,(T_w/T_{e0} \simeq 9.2)$, we imagine that a surface mass flow rate of $\dot{m}_w = 10^{-4}\rho_{e0}\mu_{e0}$ (which is typical of practical transperation or ablation cooling problems) is vectored at various angles θ_B with respect to the wall. Thus $-f_{w0} = (2\,Re_{0x})^{1/2}\,(\dot{m}w/\rho_{e0}u_{e0})\,\sin\theta_B \cong 10^{-3}$ and we can evaluate the influence of vectoring angle on the induced pressure, heat-transfer, and skin friction directly from the preceding engineering relations and Table 1. The results are shown in Table 2, from which it can be seen that both viscous interaction effects and heat transfer reduction increase very significantly with θ_B. In this example, fully-normal blowing increases the induced pressure by over 60% and enhances the corresponding skin friction increment due to viscous-inviscid interaction by three fold.

References

[1] Inger, G. R. and Swean, T. F., "Vectored Injection into Laminar Boundary Layers with Heat Transfer," *AIAA Journal*, Vol. 13, May 1975, pp. 616-622.

[2] Thyson, N. A. and Schurmann, E. H., "Blowing Effects on Pressure Interaction Associated with Cones," *AIAA Journal*, Vol. 1, Sept. 1963, pp. 150-155.

[3] Li, T. Y. and Gross, J. F., "Hypersonic Viscous Interaction on a Slender Body of Revolution and Surface Mass Transfer," Rand Corp., Santa Monica, Calif., RM-4491-ARPA, Sept. 1967.

[4] Hayes, W. D. and Probstein, R. F., *Hypersonic Flow Theory*, 1st Ed., Academic Press, N.Y., 1959, pp. 341-353.

[5] Inger, G.R. and Swean, T.F., "Hypersonic Viscous-Inviscid Interaction with Vectored Surface Mass Transfer," Virginia Polytechnic Inst. and State Univ., Blacksburg, Va., Dept. of Aerospace and Ocean Engr., Aero-012, March 1974 (AFOSR-74-0193TR, AD-775098).

[6] Maslen, S.H., "Second Approximation to Laminar Compressible Boundary Layer Flow on a Flat Plate in Slip Flow," NACA TN2818, 1952.

[7] Lees, L. and Probstein, R.F., "Hypersonic Viscous Flow Over a Flat Plate," Princeton, N.J., Princeton University Aeronautical Engineering Lab., Rept. 195, April 1952.

[8] Emmons, H.W. and Leigh, D.C., "Tabulation of the Blasius Function with Blowing and Suction," Harvard University Combustion Aerodynamic Lab., Boston, Mass., Rept. 9, 1953.

[9] Inger, G. R., "Vectored Injection into Isobaric Laminar Boundary Layer Flows," *Warme-und Stossubertragung*, Vol. 5, July 1972, pp. 201-203.

[10] Inger, G. R. and Swean, Jr., T. F., "Vectored Injection into Non-Adiabatic Boundary Layer Flows Including Incipient Separation," Virginia Polytechnic Institute and State University, Dept. of Aerospace and Ocean Engineering, Blacksburg, Va., VPI-Aero-003, June 1973.

[11] Cohen, C.B. and Reshotko, E., "Similar Solutions for the Compressible Laminar Boundary Layer with Heat Transfer and Pressure Gradient," NACA Rept. 1293, 1956.

[12] Libby, P. A. and Liu, T. M., "Further Solutions of the Faulkner Skan Equation," *AIAA Journal*, Vol. 5, May 1967, pp. 1040-1042.

[13] Kennedy, E. D., "Wake-Like Solutions of the Laminar Boundary Layer Equations," *AIAA Journal*, Vol. 2, Feb. 1964, pp. 225-231.